

DEVELOPMENT OF NANOXAFS: NEW USE OF PHOTOELECTRON EMISSION MICROSCOPE (PEEM) IN CONNECTION WITH HARD X-RAY

Over the last decade, the photoelectron emission microscope (PEEM) has been successfully developed for surface science and related nanotechnologies. PEEM is a type of electron microscope that can magnify spatial information about secondary electrons photoemitted from a surface with the lateral resolution power of several ten nanometers. Its application has been particularly carried out in combination with soft X-ray. Here, we report a new use of PEEM in connection with hard X-ray. This technique offers two possible information: one is local structure analysis at the arbitrary pixel on an observed image; another is photoelectron information from the buried layers. We are developing the "NanoXAFS" technique for local structure analysis [1,2]. The concept of this measurement technique is entirely different from conventional spatially resolving X-ray absorption fine structure (XAFS) techniques established using the Fresnel's Zone plate or microbeam because the NanoXAFS technique does not need a focused X-ray beam and all the pixels in the observed image are acquired simultaneously.

X-ray absorption intensity is proportional to the intensity of a secondary electron photoemitted from the surface, and spatial resolved information of the

secondary electron is projected on the screen of the PEEM analyzer; therefore, the intensity of each pixel in the observed image is proportional to the X-ray absorption intensity. XAFS represents element-specific information about electronic states, and the oscillatory signal in an extended range provides information about the local environment around the absorbing atom [3]. Furthermore, the excitation by hard X-rays creates high-energy Auger electrons with long penetration ranges. Thus, the combination of PEEM and hard X-ray provides spatial resolved information for the XY direction and information from the buried layers for the Z direction. Experiments were carried out at beamline **BL39XU**. Hard X-ray synchrotron radiation is available in a range of photon energies from 5 to 37 keV. PEEM SPECTOR (Elmitec, GmbH) was installed inside the experimental hutch.

We show successful examples measured on Gibeon iron meteorite at first. Gibeon iron meteorite exhibits a characteristic micrometer-sized structure known as the Widmanstätten structure that is considered a mixed multi-crystal composed of bcc-FeNi and fcc-FeNi. NanoXAFS images were continuously recorded by scanning the photon energy over the Fe and Ni *K*-absorption edges. The normalized spatial

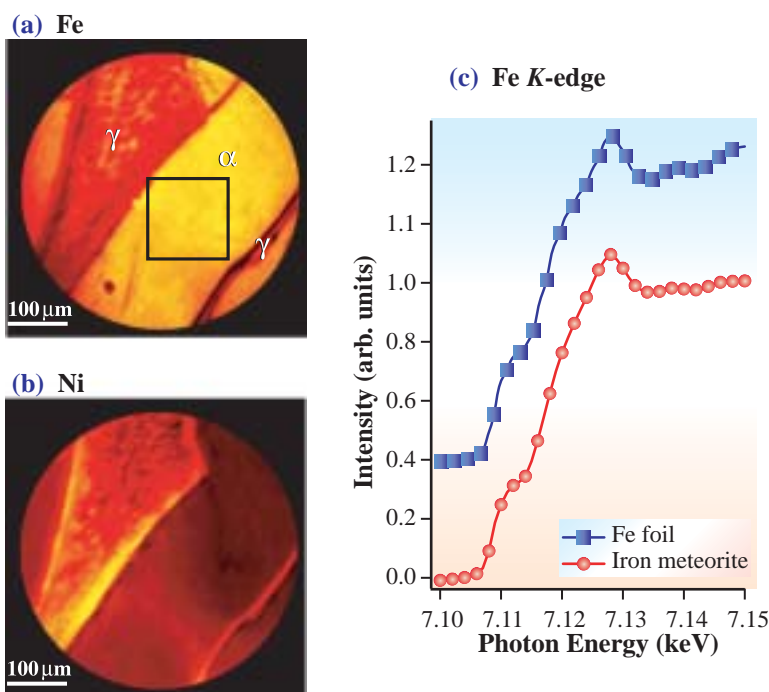


Fig. 1. Spatial distribution of XAS intensity in Gibeon iron meteorite, (a) normalized image for Fe composition (b) normalized image for Ni composition. (c) Averaged XAS intensity in iron meteorite (red line with circle) extracted from squared region in (a). Fe absorption spectrum on reference specimen of Fe foil (blue line with square).

Instrumentation & Methodology

distributions for Fe and Ni compositions are shown in Figs. 1(a) and 1(b), respectively. The Ni distribution in a thick γ lamella is spatially non-homogeneous and rapidly increases when approaching the interface. Thin γ lamellae and uneven thick γ lamellae are separated by thick γ lamellae. This is likely the result of the interatomic diffusion of Fe and Ni in the core of a mother body when an asteroid has been cooled at an extremely slow rate. The averaged XAFS spectrum for Fe extracted from the square in Fig. 1(a) is shown in Fig. 1(c) as a red line with filled circles, and the blue line with filled squares is obtained from a reference specimen of the bcc-Fe foil. The sharp crest is recognized at the absorption edge of the iron meteorite. However, the spectrum of the synthetic bcc-Fe foil also shows a similar behavior. The shape of the crest in the synthetic $\text{Fe}_x\text{Ni}_{1-x}$ system is reported to commonly show a single peak when the crystallographic structure takes bcc below 25 at.% Ni [4]. Therefore, the result of the iron meteorite suggests that the γ lamella takes the bcc structure with spatially homogeneous composition.

Next, we evaluate the probing depth of this method. We used a patterned Co thin film on a Si substrate etched by a focused ion beam (FIB). Figure 2(a) shows the schematic view of the multilayer of Pt/Co/Au/Cr deposited on the Si substrate. The thicknesses of the layers were 0.5, 50, 100 and 1 nm. Figure 2(b) shows the observed image at photon energy of 11.85 keV. The two dark square regions correspond to the Co patterns. Figure 2(c) shows the extracted NanoXAFS spectra over the Au L_{III} -edge from area 1 and area 2 marked by squares in Fig. 2(b). The former exhibits the signals from the bare Au layer, and the latter from the Au layer under the Co overlayer. We clearly see Au signals under the 50-nm-thick Co layer. The magnitude of the edge jump for the Au layer under the Co overlayer is 28% of that for the bare Au layer. To quantitatively discuss the probing depth, we used the calculation formula proposed by Erbil *et al.* [5]. This method revealed that the probing depth for total electron yield with hard X-rays is determined primarily by the penetration ranges of high-energy Auger electrons. Our calculation shows that the edge jump at Au L_{III} is 29% of that for the bare Au layer. This value is in excellent agreement with our experimental result of 28%. Using this formula, the maximum probing depth for NanoXAFS is concluded to be ten times deeper than that for conventional PEEM with soft X-ray.

Consequently, we indicate several results obtained by NanoXAFS and it has a potential to treat a wide variety of materials in surface science, nanotechnology

and planetary science. More experience will be necessary to perfect NanoXAFS.

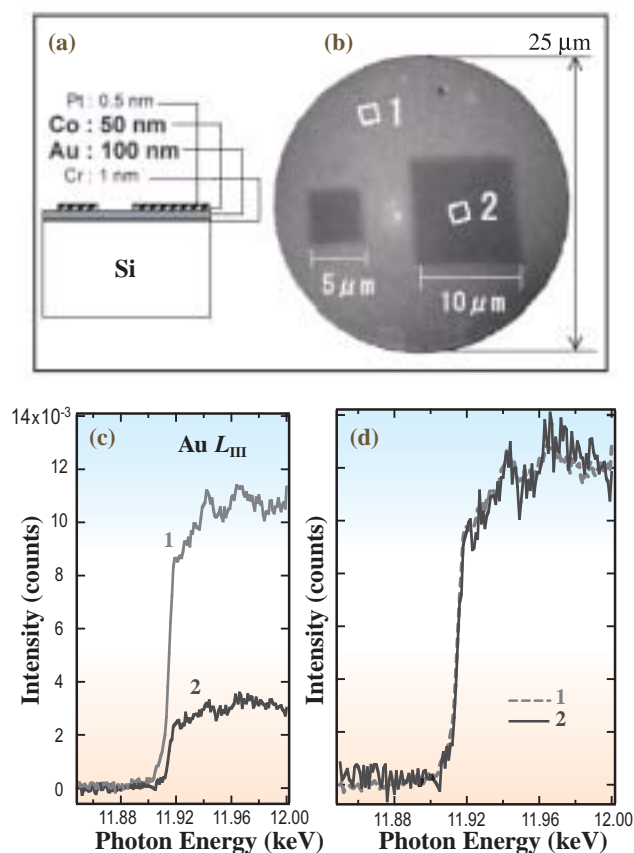


Fig. 2. (a) Schematic illustration of sample, showing its stacking sequence. (b) PEEM image of sample. The field of view is 25 μm . The sizes of the dots are 5 and 10 μm . (c) Total yield spectra near Au L_{III} edge of areas 1 and 2 marked with squares in (b). (d) The same spectra as (c) normalized to integrated intensities.

M. Kotsugi^{a,*}, T. Wakita^b and K. Ono^c

^a Hiroshima Synchrotron Radiation Center,
Hiroshima University

^b SPring-8 / JASRI

^c High Energy Acceleration Research Organization

*E-mail: kotsugi@hiroshima-u.ac.jp

References

- [1] T. Wakita *et al.*: Jpn. J. Appl. Phys. **45** (2006) 1886.
- [2] M. Kotsugi, T. Wakita, T. Taniuchi, K. Ono, M. Suzuki, N. Kawamura, M. Takagaki, M. Taniguchi, K. Kobayashi, M. Oshima, N. Ishimatsu and H. Maruyama: *e-J. Surf. Sci. Nanotech.* **4** (2006) 490.
- [3] J. Stöhr: NEXAFS Spectroscopy, Springer Verlag (Berlin).
- [4] H. Sakurai *et al.*: J. Phys. Soc. Jpn. **62** (1993) 459.
- [5] A. Erbil *et al.*: Phys. Rev. B. **37** (1988) 2450.